Validating Critical Limits of the Universal Brain Injury Criterion

Igor Szczyrba[1], **Martin Burtscher**[2], **and Rafał Szczyrba**[3]
[1]School of Mathematical Sciences, University of Northern Colorado, Greeley, CO 80639, U.S.A.
[2]Department of Computer Science, Texas State University–San Marcos, TX 78666, U.S.A.
[3]Funiosoft, LLC, Silverthorne, CO 80498, U.S.A.

Abstract— *We present results of numerical simulations that further validate the critical limits we previously proposed for our universal Brain Injury Criterion (BIC). The BIC extends the applicability of the translational Head Injury Criterion (HIC) to arbitrary head motions by reformulating the acceleration-based HIC formula in terms of the energy transferred locally from the skull to the brain. Our simulations are based on a generalization of the Kelvin-Voigt (K-V) Closed Head Injury model that includes a nonlinear strain-stress relation. We validate the proposed BIC limits against (i) the critical limit $HIC_{15} = 700$, (ii) the Diffuse Axonal Injury Tolerance Criterion (DAITC) for head rotations that has been derived from the K-V model and from experiments with animal brains, and (iii) recent experimental data on strain levels leading to permanent neuronal damage. Our results imply that for head rotations about various fixed axes, the critical BIC_{15} limits coincide with the HIC_{15} critical limit and are in agreement with the DAITC thresholds.*

Keywords: brain injury, universal critical limits

1. Introduction

In previous work [1], [2], [3], we have introduced a universal Brain Injury Criterion (BIC) that allows assessing Closed Head Injury (CHI) caused by arbitrary traumatic head motions. Our approach is based on the assumption that if energy is transferred *locally* from the skull to the brain in a similar way, the likelihood and severity of a brain injury in a given location should be similar in any traumatic scenario, including traumatic head translations.

This article makes the following contributions: First, to the best of our knowledge, we are the first to establish that the way in which energy is transferred locally from the skull to the brain can play a crucial role in determining the likelihood and severity of a brain injury during arbitrary traumatic head motions. Specifically, we consider the rate at which energy (i.e., power) is transferred to the brain per unit mass from the moving skull as well as the rate of power transferred to the brain (i.e., whether energy is transferred to the brain in an accelerated or constant way).

Second, by using the energy/power transferred locally from the skull to the brain during traumatic head motions as a predictor of a brain injury, we introduce a 'common denominator' for assessing the severity and likelihood of the injury appearing as a result of traumatic head translations and rotations. This makes it possible to establish a direct link between the translational and rotational critical limits introduced by other researchers.

Third, we demonstrate how the operator norm of the strain matrix can be used to evaluate the time evolution of the spatial distribution of the maximal strain in the brain matter.

Fourth, by numerically simulating various traumatic scenarios using our nonlinear CHI model, we show that, for head rotations about *fixed* axes lasting for 0.015s, the BIC critical limits (i) do not depend in an essential way on the position of the rotational axis, (ii) coincide with the new critical limit $HIC_{15} = 700$, and (iii) are in agreement with the existing rotational Diffuse Axonal Injury thresholds.

1.1 Derivation of the BIC formula

Based on our assumption regarding the local transfer of energy from the skull to the brain, we derive the BIC formula from the well-established translational Head Injury Criterion (HIC) formula:

$$HIC_{1000T} = \max A^{2.5} T, \tag{1}$$

where T is a time subinterval of the head's translational acceleration time, A is the average (over T) of the acceleration magnitude's absolute value, and the maximum is taken over all subintervals T.

Specifically, for monotone accelerations, we express A in terms of the energy E and the power P as follows:

$$A = \sqrt{2}P \big/ \big(\sqrt{(E(t_2)} + \sqrt{E(t_1)}\,\big), \tag{2}$$

where $E(t)$ denotes the average kinetic energy per unit mass at time t transferred to the brain surface from a translated skull, and $P = |E(t_2) – E(t_1)|/T$ is the absolute value of the average power transferred per unit mass to the brain in the time interval $T = t_2 - t_1$, *cf.* [1] for details.

The reformulation of the acceleration A in terms of energy and power allows us to generalize the applicability of the HIC formula (1) to arbitrary traumatic head motions, i.e., to introduce the following formula:

$$BIC_{1000T} = \max \left(\frac{\sqrt{2}P}{\sqrt{2E(t_1)} + \sqrt{2E(t_2)}} \right)^{2.5} T. \tag{3}$$

Let us note that, contrary to the case of a head translation, during an arbitrary head motion, energy is transferred non-uniformly from the skull to the brain, i.e., both E and P depend not only on the time t but also on the localization of the brain parcels. For instance, during a head rotation about a *fixed* axis, the energy transferred to the brain is negligible near the axis because the magnitude of the rotational velocity is very small there. Hence, in case of an arbitrary traumatic head motion, the maximum in the formula (3) should be taken not only over all time intervals T but also over the entire brain surface.

If, for a time interval $T{=}t_2{-}t_1$ for which the maximum in (3) is assumed, the velocity of an acceleration pulse is zero at t_1 or t_2, the BIC formula (3) can be simplified to become a function of only the average power P and the duration of the acceleration time T:

$$BIC_{1000T} = \max\, 2P(2P/T)^{0.25}, \tag{4}$$

where the ratio P/T approximates the rate at which power is transferred to the brain. Thus, our BIC formula (4) exposes a new role that is possibly played in the creation of brain injuries by an accelerated delivery of power from the skull to the brain (second temporal derivative of energy).

1.2 Rotations about fixed axes

In the case of accelerated head rotations about *fixed* axes (which we focus on in this study), the requirement that the maximum should be taken over the entire brain surface can be relaxed by considering only a thin strip of the brain's surface located along the boundary of the 2D brain cross section that is perpendicular to the rotational axis and is characterized by the *highest* value of tangential velocity.

Moreover, if the magnitude of this tangential velocity over time is the same as the magnitude of the translational velocity characterizing a head's accelerated translation, the likelihood and severity of a brain injury appearing in this brain cross-section should be similar to the likelihood and severity of an injury when the head is translated since the local transfer of energy along the cross section's boundary is practically identical in both traumatic scenarios. Consequently, it should be possible to directly use the critical HIC limits introduced in [4], [5] to derive the critical BIC limits for traumatic head rotations about fixed axes.

1.3 Correlation between translational and rotational brain injury criteria

In deriving BIC critical limits for traumatic head rotations about fixed axes, our approach allows us to also use the rotational critical limits introduced by the Diffuse Axonal Injury Tolerance Criterion (DAITC). DAITC has been developed in 1992 based on experiments with baboon brains and the *linear* viscoelastic Kelvin-Voigt (K-V) CHI model, *cf.* [6]. The DAITC is expressed in terms of the peak rotational acceleration about a *fixed* rotational axis positioned centroidally, and the peak change of the rotational velocity's magnitude.

In fact, considering how energy is transferred locally from the skull to the brain in traumatic situations as a brain injury predictor allows us to link the translational critical HIC limits with the rotational critical DAITC limits. For instance, the maximum translational acceleration of a triangularly shaped acceleration pulse characterized by the critical HIC_{15}=700 limit equals 150g=1,472m/s^2 and the corresponding peak change in the velocity is 5.4m/s, *cf.* Fig. 2 in Section 3.

If the same tangential pulse is used to centroidally rotate an adult human head with an 'average radius' of 0.1m about a fixed axis, the maximum rotational acceleration equals 14,460rad/s^2 and the peak change in the rotational velocity magnitude equals 55rad/s. This corresponds to a point that is near the critical region defined by the DAITC analytic model's threshold curve and is inside the critical region defined by the DAITC physical model, *cf.* Fig. 5 in [6].

2. Generalized Kelvin-Voigt CHI model

We further validate the critical BIC limits by conducting simulations using our numerical nonlinear CHI model that generalizes the K-V model used to derive DAITC.

2.1 Nonlinear stress-strain relation

Following experimental data obtained over the last two decades, *cf.* [7], [8], [9], we include a *nonlinear* stress-strain relation in our generalization of the K-V CHI model. Thus, our computational model utilizes the following Partial Differential Equations (PDEs) describing the propagation of shear waves in incompressible viscoelastic materials:

$$\frac{\partial \mathbf{v}(\mathbf{x},t)}{\partial t} = \triangle(c^2(\mathbf{x},t)\mathbf{u}(\mathbf{x},t) + \nu\,\mathbf{v}(\mathbf{x},t)),$$
$$\frac{\partial \mathbf{u}(\mathbf{x},t)}{\partial t} = \mathbf{v}(\mathbf{x},t), \quad \nabla{\cdot}\mathbf{v}(\mathbf{x},t) = 0, \tag{5}$$

where $\mathbf{v}(\mathbf{x},t) \equiv (v_1(\mathbf{x},t), v_2(\mathbf{x},t), v_3(\mathbf{x},t))$ with $\mathbf{x} \equiv (x_1, x_2, x_3)$ represents the brain matter velocity vector field at time t in an *external* coordinate system, $\mathbf{u}(\mathbf{x},t)$ is the corresponding displacement vector field, $c(\mathbf{x},t)$ describes the brain's shear wave velocity that depends on the distribution of strain in the brain matter, and ν is the brain's kinematic viscosity.

Specifically, based on experimental data reported in [7], we model the stress-strain relation as an exponential function, i.e., we set

$$c(\mathbf{x},t) \equiv c \cdot \exp(r \cdot s(\mathbf{x},t)), \tag{6}$$

where $c \equiv \sqrt{G/\delta}$ denotes the basic shear wave velocity in the absence of strain (with G and δ being the brain matter shear modulus and density, respectively), $s(\mathbf{x},t)$ describes the time

evolution of the spatial distribution of the maximum strain within the brain matter, and r is a coefficient determining how the brain matter stiffens under strain.

Since there are no experimental data on the brain matter's strain-stress relation for very large strains, we make the assumption that for strains larger than m%, e.g., exceeding $m = 50\%$, the shear wave velocity $c(\mathbf{x}, t)$ given by (6) 'saturates', i.e., it smoothly becomes proportional to the basic velocity c.

2.2 Spatial distribution of maximal strain

To find the spatial distribution $s(\mathbf{x}, t)$ of the maximal strain, we evaluate the components of the matrix:

$$\mathbf{S}(\mathbf{x}, t) \equiv \nabla \cdot \mathbf{U}(\mathbf{x}, t) + \mathbf{I} \equiv \partial \mathbf{U} \frac{\partial}{\mathbf{x}}(\mathbf{x}, t) + \mathbf{I}, \qquad (7)$$

where $\mathbf{U}(\mathbf{x},t) \equiv (\mathrm{U}_1(\mathbf{x},t),\mathrm{U}_2(\mathbf{x},t),\mathrm{U}_3(\mathbf{x},t))$ denotes the brain matter's displacement vector field *relative* to the moving skull, $\nabla \cdot \mathbf{U}(\mathbf{x}, t)$ is the strain matrix of this field, and $\mathbf{I}$ is the identity matrix in 3D.

The diagonal terms in the strain matrix $\nabla \cdot \mathbf{U}(\mathbf{x},t)$ determine the contribution of the partial derivatives to the brain deformation by evaluating the brain matter's *strain* with regard to the directions of the base vectors used, whereas the partial derivatives in the non-diagonal terms determine their contribution to the brain deformation by evaluating the *total deformation* of the brain matter.

Adding *one* to the diagonal terms in (7) puts all partial derivatives on 'equal footing', i.e., enables us to evaluate the maximal total deformation in each point $\mathbf{x}$ of the brain at time t by using the operator norm $\| \ \|_O$ of the matrix $\mathbf{S}(\mathbf{x}, t)$. Next, by subtracting *one* from this maximal total deformation, we obtain the spatial distribution of the maximal strain at time t. Thus, the function $s(\mathbf{x}, t)$ is given by:

$$s(\mathbf{x}, t) \equiv ||\mathbf{S}(\mathbf{x}, t)||_O - 1 \equiv \sup||\mathbf{S}(\mathbf{x}, t) \cdot \mathbf{y}|| - 1, \qquad (8)$$

where $\mathbf{y} \equiv (y_1, y_2, y_3)$, $||\ ||$ denotes the vector norm in 3D, and the supremum is taken over all vectors $\mathbf{y}$ with $||\mathbf{y}|| = 1$. One can easily check that:

$$s(\mathbf{x}, t) \leq ||\nabla \cdot \mathbf{U}(\mathbf{x}, t)||_O, \qquad (9)$$

i.e., the operator norm $\|\nabla \cdot \mathbf{U}(\mathbf{x}, t)\|_O$ of the strain matrix provides an upper bound for the function $s(\mathbf{x}, t)$ describing the spatial distribution of the maximal strain.

3. Simulation setup

In this paper, we present simulation results of head translations in a fixed direction as well as of head rotations about certain fixed rotational axes. As mentioned above, this allows us to directly verify the results of our numerical simulations using the HIC and DAITC critical limits.

In both of these scenarios the forces applied to the head have one zero component, and consequently, one component of the 3D solutions is zero. Therefore, it suffices to solve PDEs (5)−(8) only in 2D brain cross sections near which the transfer of energy from the skull to the brain is the largest.

Thus, for forward head translations and rotations, we present the results of our simulations in a sagittal brain cross section that is positioned near the falx cerebri, whereas for lateral head rotations, we present the results in a coronal brain cross section that is positioned near the brain's center of mass and that includes the falx cerebri.

3.1 Skull-brain facsimile

As solution domains, we use 2D facsimiles of the skull-brain cross sections consisting of three layers: (i) the skull and dura layer, (ii) the Cerebro Spinal Fluid (CSF) layer, and (iii) the brain matter layer, *cf.* Fig 1. Specifically, we model the skull and the dura mater as a solid body layer, the $4{\cdot}10^{-3}$m thick CSF layer representing the pia-arachnoid complex with the fluid is modeled as an incompressible elastic medium, and the brain matter is modeled as an incompressible viscoelastic medium.

Since there exist no conclusive experimental data on how the stress depends on the strain in the gray matter, the brain matter is assumed to be homogenous having the physical characteristics of the white matter.

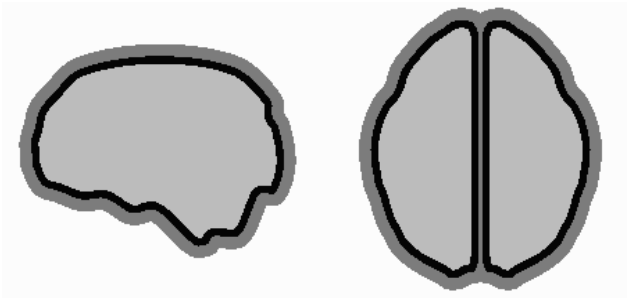

Fig. 1
THE THREE-LAYER SAGITTAL AND CORONAL HEAD CROSS SECTIONS SOLID BODY SKULL AND DURA MATER - DARK GRAY, ELASTIC CSF COMPLEX - BLACK; VISCOELASTIC HOMOGENOUS BRAIN - LIGHT GRAY

Experimental data in [7], [10−17] imply that the shear wave velocity in the white matter is approximately 1m/s, the stiffening coefficient $0.5 \leq r \leq 2.5$, the brain's viscosity $0.009\mathrm{m}^2/\mathrm{s} \leq \nu \leq 0.017\mathrm{m}^2/\mathrm{s}$, and neurons can sustain mechanical strain up to 80%.

According to [18], the CSF layer is predominately modeled as an incompressible elastic medium with a shear modulus G_{CSF} as low as 200PA, which reflects the role of the CSF in reducing the strain within the brain matter [19]. The simulation results presented here are obtained with the following values for the constants in the system (5)−(8): c=1m/s, ν=$0.013\mathrm{m}^2$/s, r=1.4, m=50%, G_{CSF}=225PA.

3.2 Acceleration loads used

We simulate forward head translations and forward head rotations about fixed horizontal axes positioned at the head's center of mass, the chin, the neck, and the abdomen as well as lateral head rotations about fixed vertical axes positioned at the head's center of mass, the skull, and at some distances outside of the skull.

We present simulation results obtained using a triangular acceleration load with the acceleration time $T = 0.015$s and the tangential acceleration and velocity magnitudes corresponding to $HIC_{15} = BIC_{15}$ ranging from 100 to 1000. Fig. 2 depicts the dynamic characteristics of the critical load used with $HIC_{15} = BIC_{15} = 700$.

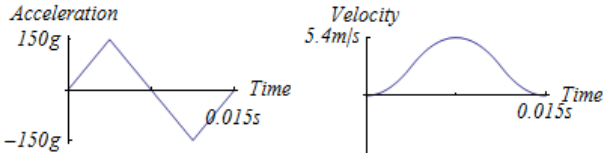

Fig. 2

DYNAMIC CHARACTERISTICS OF THE ACCELERATION LOAD WITH $HIC_{15} = BIC_{15} = 700$

4. Simulation results

To evaluate the possible severity of a brain injury, we find the absolute maximum $s_{\max}$ of the function $s(\mathbf{x}, t)$, i.e., the maximum strain value attained in a given brain cross section during or some time after the head is accelerated.

4.1 Simulations of forward head translations

Table 1 depicts the values of $s_{\max}$ attained in the coronal and sagittal brain cross sections in our simulations of forward head translations under loads characterized by four HIC_{15} values ranging between 100 and 1000.

HIC_{15}	100	400	700	1000
coronal	10%	20%	25%	27%
sagittal	17%	27%	35%	38%

Table 1

MAXIMAL STRAIN $s_{\max}$ IN THE CORONAL AND SAGITTAL CROSS SECTIONS ATTAINED DURING OR AFTER FORWARD HEAD TRANSLATIONS WITH HIC_{15} RANGING BETWEEN 100 AND 1000

Experiments imply that neurons sustain permanent damage due to a chemical imbalance when stretched by 25%-30% [6], [7], [20]. For the $HIC_{15} = 700$ load, the average of the $s_{\max}$ values attained in both brain cross sections equals 30%. Thus, our translational results are in good agreement with this critical HIC limit, which validates the predictions of our computational CHI model.

The disparity between the $s_{\max}$ values in the coronal and sagittal brain cross sections are most likely due to the fact that the simulations with the sagittal cross section do not take into account the impact of the falx cerebri, which seems to lower the maximal strain, *cf.* [6].

4.2 Simulations of head rotations

Diffuse Axonal Injuries (DAI) appear predominantly as a result of rapid head rotations, *cf.* [21]. To derive critical BIC values that can be used to assess the severity and likelihood of DAI, we conduct numerous simulations of head rotations under loads characterized by a variety of BIC values.

Table 2 depicts the values $s_{\max}$ attained under BIC_{15} loads ranging from 100 to 1000 in the sagittal brain cross section during or after forward head rotations about fixed horizontal axes positioned at the head's center of mass, the chin, the neck, and the abdomen.

$s_{\max}$ values in sagittal cross section	BIC_{15}			
forward rotation about fixed axis at	100	400	700	1000
head's center of mass	17%	32%	37%	39%
chin	17%	32%	36%	43%
neck	13%	29%	35%	40%
abdomen	19%	29%	36%	39%

Table 2

MAXIMAL STRAIN $s_{\max}$ IN THE SAGITTAL CROSS SECTION ATTAINED DURING OR AFTER FORWARD HEAD ROTATIONS ABOUT VARIOUS HORIZONTAL AXES WITH BIC_{15} VALUES BETWEEN 100 AND 1000

Table 3 shows the values $s_{\max}$ attained under the same BIC_{15} loads but in the coronal brain cross section when the head is rotated laterally, counter-clockwise about fixed vertical axes positioned at the head's center of mass, the skull, 0.1m from the skull, and 0.2m from the skull.

$s_{\max}$ values in coronal cross section	BIC_{15}			
lateral rotation about fixed axis at	100	400	700	1000
head's center of mass	11%	25%	39%	40%
skull	17%	35%	40%	41%
0.1m from the skull	16%	35%	40%	40%
0.2m from the skull	15%	30%	35%	37%

Table 3

MAXIMAL STRAIN $s_{\max}$ IN THE CORONAL CROSS SECTION ATTAINED DURING OR AFTER LATERAL HEAD ROTATIONS ABOUT VARIOUS VERTICAL AXES WITH BIC_{15} VALUES BETWEEN 100 AND 1000

These simulation results provide maximal strain values $s_{\max}$ that are slightly higher than (but still in line with) the values obtained for head translations. Let us note, however, that during rapid head rotations the absolute maxima $s_{\max}$ of strain are, in general, attained in a pointwise manner in very small regions of the brain matter during a very short period of time lasting for 0.01s to 0.02s.

Such localized high strain values lasting for such short periods of time should only be used to obtain an upper bound

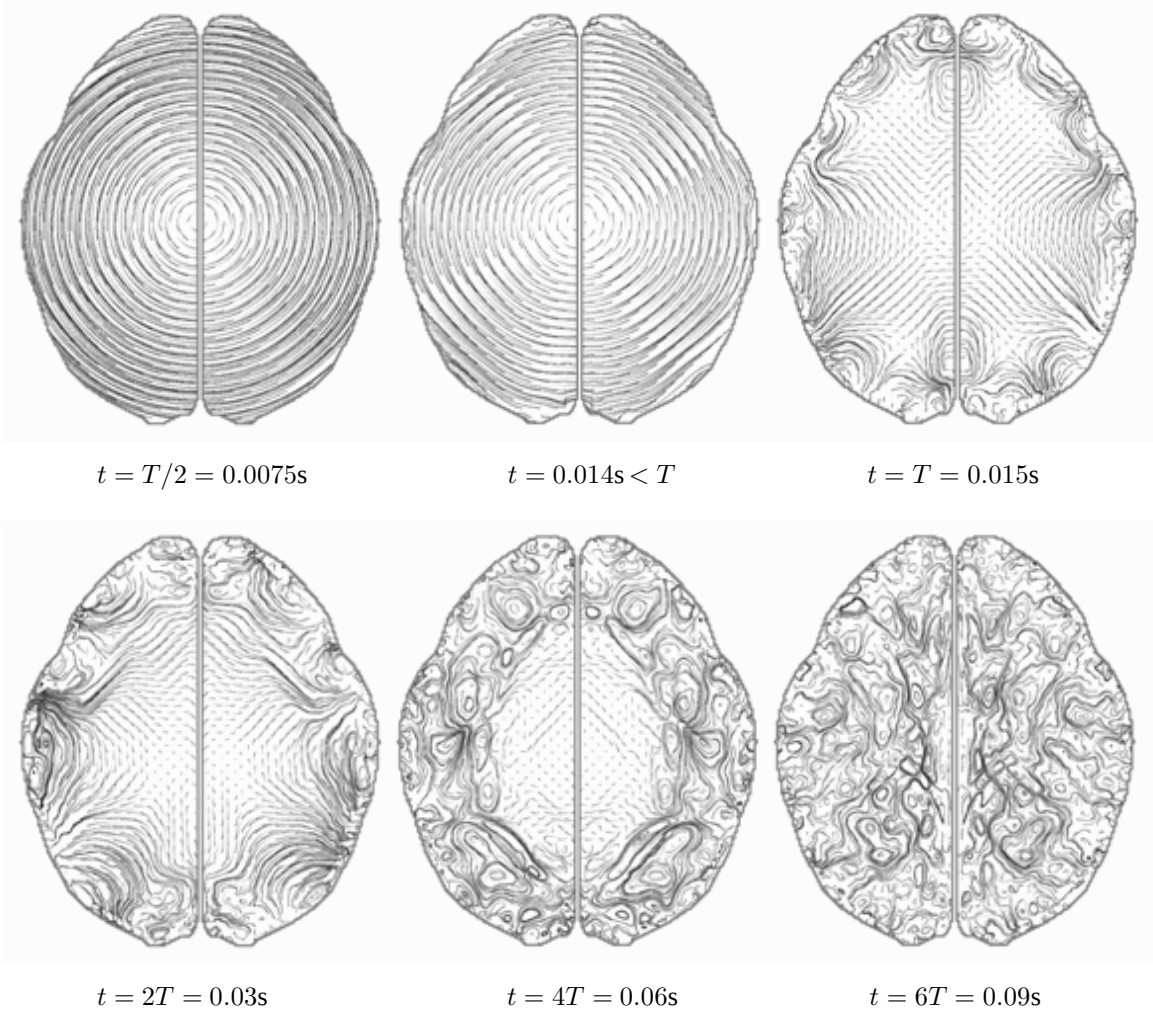

Fig. 3

TIME EVOLUTION OF THE VELOCITY CURVED VECTOR FIELD V(x_1, x_2, t) RELATIVE TO THE SKULL IN THE CORONAL BRAIN CROSS SECTION DURING AND AFTER A LATERAL HEAD ROTATION WITH $BIC_{15} = 700$ ABOUT A VERTICAL AXIS POSITIONED AT THE BRAIN'S CENTER OF MASS

estimate for predicting DAI likelihood and severity, since the loss of axonal transport in a single axon does not properly reflect the spatial scattering of DAI [22].

Instead, the Cumulative Strain Damage Measure (CSDM) introduced in [23] has been accepted as a good DAI predictor [24]. An initial analysis of our simulation results from the point of view of the CSDM suggests that the critical HIC value of 700 can be used as the BIC critical value for head rotations about fixed axes and as a starting point for establishing critical BIC limits for arbitrary head rotations.

Since commercial software cannot adequately depict highly localized oscillations of vector fields, we have developed animated Curved Vector Field (CVF) plots [25]. CVF plots use curved, dark-to-light shaded lines instead of arrows to indicate the motion's direction. They provide a good depiction of vectors and portray potential trajectories of brain parcels. Animated versions of our CVF plots are available at http://www.funiosoft.com/brain/ in form of MPEG movies.

Fig. 3 (resp. 4) depicts time snapshots of CVF animations representing the brain matter's velocity vector field V(x_1, x_2, t) *relative* to the moving skull at various times t in the coronal (resp. sagittal) 2D brain cross section when the head is rotated laterally, counter-clockwise (resp. forward) under the $BIC_{15} = 700$ load about an axis positioned at the brain's center of mass.

The highly localized brain matter oscillations depicted in Figs. 3 and 4 create multiple local strain maxima that are scattered over the entire brain cross section.

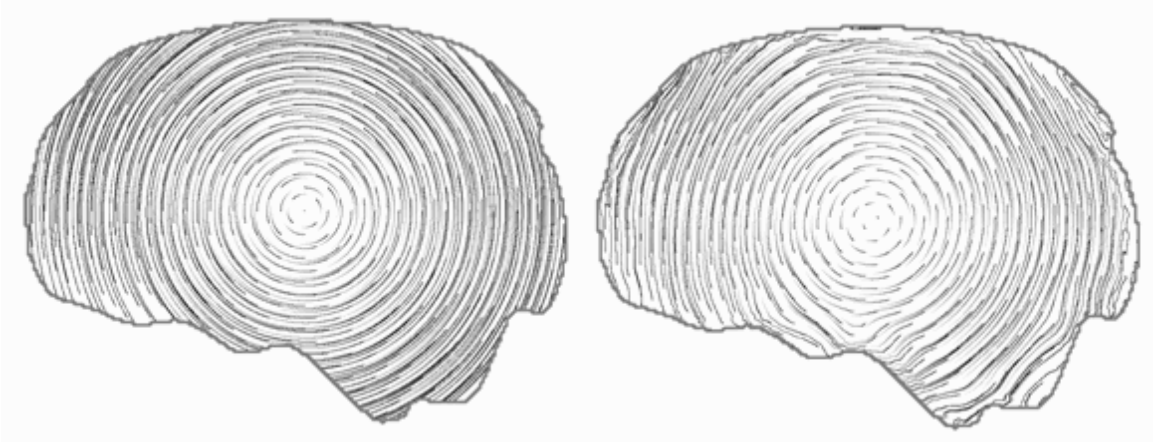

$t = T/2 = 0.0075\text{s}$ $t = 0.014\text{s} < T$

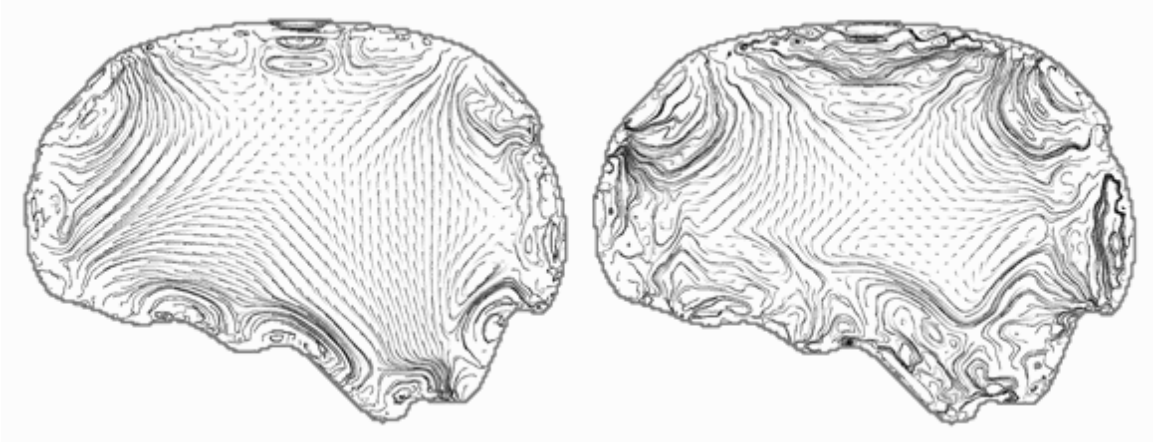

$t = T = 0.015\text{s}$ $t = 2T = 0.03\text{s}$

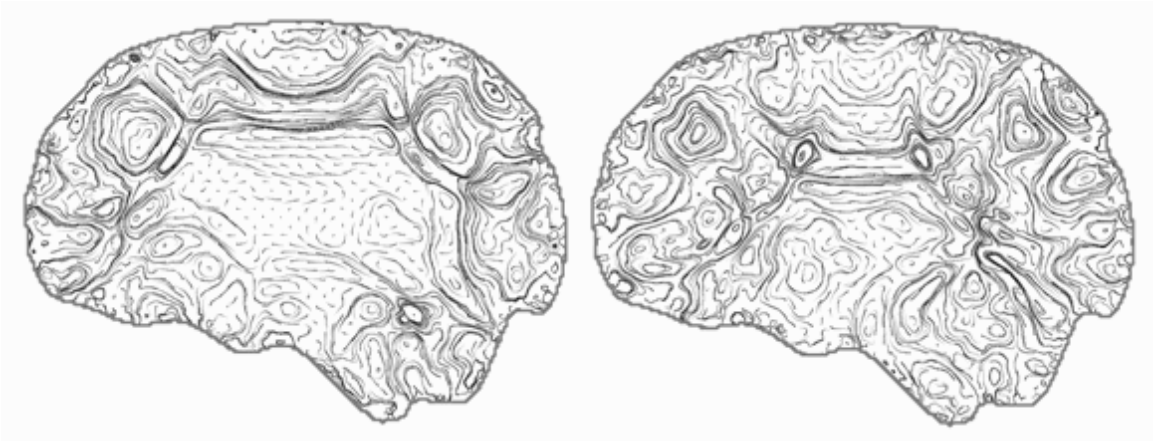

$t = 4T = 0.06\text{s}$ $t = 5T = 0.075\text{s}$

Fig. 4

TIME EVOLUTION OF THE VELOCITY CURVED VECTOR FIELD $\mathrm{V}(x_1, x_2, t)$ RELATIVE TO THE SKULL IN THE SAGITTAL BRAIN CROSS SECTION DURING AND AFTER A FORWARD HEAD ROTATION WITH $BIC_{15} = 700$ ABOUT A HORIZONTAL AXIS POSITIONED AT THE BRAIN'S CENTER OF MASS

Note that, in the case of the lateral head rotation, the brain matter oscillations 'spread' throughout the entire cross section at a later time in comparison to the forward head rotation. This shows again that the falx cerebri plays a role in shaping the DAI features.

5. Conclusions

Our idea that the severity and likelihood of brain injuries can be assessed, regardless of whether a head is translated or rotated, based on the analysis of how the energy is locally transferred from the skull to the brain enables us to develop a universal Brain Injury Criterion applicable for arbitrary traumatic head motions. Our approach further allows to correlate the new Head Injury Criterion critical limits derived in [4], [5] with the Diffuse Axonal Injury Tolerance Criterion critical values established in [6].

The results from numerical simulations based on our viscoelastic Closed Head Injury model that includes a nonlinear strain-stress relation imply that, for centroidal and non-centroidal head rotations about *fixed* axes with an acceleration time period $T = 0.015$s, the critical BIC_{15} limits:

- do not depend in an essential way on the position of the fixed rotational axis,
- coincide with the new critical $HIC_{15} = 700$ limit, and
- are in agreement with the critical limits implied by the DAITC threshold curves.

These results suggest that the critical $BIC_{15} = 700$ limit may be valid for arbitrary traumatic head motions.

6. Acknowledgment

The authors would like to thank Intel Corporation for providing two multiprocessor servers that were used for conducting a portion of the numerical simulations presented in this article.

References

[1] I. Szczyrba, M. Burtscher, and R. Szczyrba, "A Proposed New Brain Injury Tolerance Criterion Based on the Exchange of Energy Between the Skull and the Brain," in *Proc. 2007 Summer Bioengineering Conf.*, American Society of Mechanical Engineers, SBC 2007-171967, 2007.

[2] I. Szczyrba, M. Burtscher, and R. Szczyrba, "Computational Modeling of Brain Dynamics during Repetitive Head Motions," in *Proc. 2007 Conf. on Modeling, Simulation and Visualization Methods*, pp. 143-149, CSREA Press 2007.

[3] I. Szczyrba, M. Burtscher, and R. Szczyrba, "On the Role of a Nonlinear Stress-Strain Relation in Brain Trauma," in *Proc. 2008 Conf. Bioinformatics and Computational Biology*, vol. 1, pp. 265-271, CSREA Press 2008.

[4] M. Kleinberger *et al.*, "Development of Improved Injury Criteria for the Assessment of Advanced Automotive Restraint Systems," (1998) The NHTSA website. [Online]. Available: http://www-nrd.nhtsa.dot.gov/pdf/nrd-11/airbags/criteria.pdf

[5] R. Eppinger *et al.*, "Development of Improved Injury Criteria for the Assessment of Advanced Automotive Restraint Systems-II," (2000) The NHTSA website. [Online]. Available: http://www-nrd.nhtsa.dot.gov/pdf/nrd-11/airbags/finalrule_all.pdf

[6] S. S. Margulies, and L. Thibault, "A Proposed Tolerance Criterion for Diffuse Axonal Injury in Man," *J. of Biomechanics*, vol. 25, pp. 917-923, 1992.

[7] B. R. Donnelly, and J. Medige, "Shear Properties of Human Brain Tissue," *J. of Biomechanical Engineering*, vol. 119, pp. 423-432, 1998.

[8] E. G. Takhounts, J. R. Crandall, and K. Darvish, "On the Importance of Nonlinearity of Brain Tissue under Large Deformations," *Stapp Car Crash J.*, vol. 47, pp. 79-92, 2003.

[9] S. Mehdizadeh, *et al.*, "Comparison between Brain Tissue Gray and White Matters in Tension Including Necking Phenomenon," *American J. of Applied Sciences*, vol. 5, no. 12, pp. 1701-1706, 2008.

[10] G. T. Fallenstein, V. D. Hulce, and J. W. Melvin, "Dynamic Material Properties of Human Brain Tissue," *J. of Biomechanics*, vol. 2, pp. 217-226, 1969.

[11] C. Ljung, "A Model for Brain Deformation Due to Rotation of the Skull," *J. of Biomechanics*, vol. 8, pp. 263-274, 1975.

[12] Y. Tada, and T. Nagashima, "Modeling and Simulation of Brain Lesions by the Finite-Element Method," *IEEE Engineering in Medicine and Biology*, pp. 497-503, 1994.

[13] B. R. Donnelly, "Brain tissue material properties: A comparison of results. Biomechanical research: Experimental and computational," in *Proc. 26th Int. Workshop*, pp. 47-57, 1998.

[14] K. Paulsen, *et al.*, "A Computational Model for Tracking Subsurface Tissue Deformation During Stereotactic Neurosurgery," *IEEE Transactions on Biomechanical Engineering*, vol. 46, pp. 213-225, 1999.

[15] J. A. Wolf, *et al.*, "Calcium Influx and Membrane Permeability in Axons after Dynamic Stretch Injury in Vitro," *J. of Neurotrauma*, vol. 16, p. 966, 1999.

[16] A. Bain, and D. Meaney, "Tissue-Level Thresholds for Axonal Damage in an Experimental Model of Central Nervous System White Matter Injury," *J. of Biomechanical Engineering*, vol. 122, pp. 615-622, 2000.

[17] A. Bain, *et al.*, "Dynamic Stretch Correlates to Both Morphological Abnormalities and Electrophysiological Impairment in a Model of Traumatic Axonal Injury," *J. of Neurotrauma*, vol. 18, pp. 499-511, 2001.

[18] J. Xin, H. K. Yang, and A. J. King, "Mechanical properties of bovinepia-arachnoid complex in shear," *J. of Biomechanics*, vol. 44 pp. 467-474, 2011.

[19] Y. H. Chu, "Finite Element Analysis of Traumatic Brain Injury," 2002 [Online]. Available: at: http://www.ruf.rice.edu/ preors/Chu-YH.pdf

[20] Y. Matsui, and T. Nishimoto, "Nerve Level Traumatic Brain Injury in Vivo/in Vitro Experiments," *Stapp Car Crash J.*, vol. 54, pp. 197-210, 2010.

[21] J. Meythaler, "Amantadine to Improve Neurorecovery in Traumatic Brain Injury-associated Diffuse Axonal Injury," *J. of Head Trauma and Rehabilitation*, vol. 17, no. 4, pp. 303-313, 2002.

[22] T. A. Gennarelli, *et al.*, "Diffuse axonal injury and traumatic coma in the primate," *Annals of Neurology*, vol. 12, no. 6, pp. 564-574, 1982.

[23] F. A. Bandak, and R. H. Eppinger, "A three-dimensional finite element analysis of the human brain under combined rotational and translational accelerations," in *Proc. 38th Stapp Car Crash Conf.*, pp. 145-163, 1994.

[24] E. G. Takhounts, *et al.*, "Investigation of Traumatic Brain Injuries Using the Next Generation of Simulated Injury Monitor (SIMon) Finite Element Head Model," *Stapp Car Crash J.*, vol. 52, pp. 1-31, 2008.

[25] M. Burtscher, and I. Szczyrba, "Numerical Modeling of Brain Dynamics in Traumatic Situations — Impulsive Translations," in *Proc. 2005 Conf. on Mathematics and Engineering Techniques in Medicine and Biological Sciences*, pp. 205-211, CSREA Press 2005.